

“A study of two dimensional heat conduction in exchanger tubes of non-circular cross-section”

Santosh Kumar Rana



Department of Mathematics

National Institute of Technology Rourkela

“A study of two dimensional heat conduction in exchanger tubes of non-circular cross-section”

A dissertation submitted in partial fulfillment

of the requirements of the degree of

Master of Science

in

Mathematics

by

Santosh Kumar Rana

(Roll Number: 411MA5113)

under the supervision of

Prof. Jugal Mohapatra



May, 2016

Department of Mathematics
National Institute of Technology Rourkela



Department of Mathematics
National Institute of Technology Rourkela

Supervisor's Certificate

This is to certify that the work presented in the dissertation entitled "*A study of two dimensional heat conduction in exchanger tubes of non-circular cross-section*" submitted by *Santosh Kumar Rana*, Roll Number 411MA5113, is a bonafied research carried out by him under my supervision and guidance in partial fulfillment of the requirements of the degree of *Master of Science in Mathematics*. This dissertation has not been submitted earlier for any degree or diploma to any institute or university in India or abroad.

Dr. Jugal Mohapatra
Assistant professor
Department of Mathematics

Dedication

I dedicate this work
to
my parents.

Santosh Kumar Rana
411MA5113

Declaration of Originality

I, *Santosh Kumar Rana*, Roll Number *411MA5113* hereby declare that this dissertation entitled “A study of two dimensional heat conduction in exchanger tubes of non-circular cross-section” presents the bonafied research work carried out by me as a master’s student of NIT Rourkela. Any contribution made to this research by others, with whom I have worked at NIT Rourkela or elsewhere, is explicitly acknowledged in the dissertation. The works of other authors cited in this dissertation have been duly acknowledged under the sections “Bibliography”. I have also submitted my research records to the scrutiny committee for evaluation of my dissertation.

I am fully aware that in case of any non-compliance detected in future, the Senate of NIT Rourkela may withdraw the degree awarded to me on the basis of the present dissertation.

May 16, 2016
NIT Rourkela

Santosh Kumar Rana
411MA5113

Acknowledgment

I would like to take this opportunity to thank all the individuals without whose support and guidance I could not have completed this project in the stipulated period of time. I, wholeheartedly, acknowledge the intellectual stimulation of my esteemed guides Prof. Jugal Mohapatra, (Assistant Professor, Department of Mathematics). Special thanks to Prof. Manoj Kumar Moharana (Assistant Professor, Mechanical Department) for his continuous help and guidance throughout the project in spite of his busy work schedule. They helped me out in understanding the subject well and always stood beside me whenever I needed their help. It is the result of their sincere co-operation that I finished my project in the stipulated time.

I am highly indebted to Department of Mathematics for providing necessary information and infrastructure regarding the project and also for their support in completing the project.

I am obliged to all my friends for their friendships and encouragements. Finally, the thesis would not have been completed without the support of the most important people in my life. I sincerely wish to thank my parents for their unconditional love and constant encouragement.

May 12, 2016
NIT Rourkela

Santosh Kumar Rana
Roll Number: 411MA5113

Abstract

Two types of heat conduction problems have been investigated in this literature. Firstly, the steady state heat conduction through a two dimensional domain of both inner and outer noncircular cross-section whose inner and outer surface are kept at constant but different temperatures and it is solved by using a two dimensional semi-analytic technique called boundary collocation method. In the second case, the steady state heat conduction through the same two dimensional domain whose inner surface is kept at a constant temperature and outer surface is subjected to convective condition is solved using boundary collocation method. Some of the boundary conditions are applied to find the generalised solution of the governing differential equation and the rest of the boundary conditions are used via boundary collocation method for numerical solution. In the boundary collocation method, equal number of points on the inner boundary and on the outer boundary are considered and then necessary numerical method has been adopted to get the complete solution.

Keywords: Heat conduction; convection; boundary collocation method; conduction shape factor; heat exchanger tube.

Nomenclature

R =dimensionless radius variable

rs_i =inner surface distance from the origin of the axes

rs_o = outer surface distance from the origin of the axes

M =number of symmetry about π

N =half of the total number of collocation points

h = convective heat transfer coefficient, W/m^2K

K_t =thermal conductivity, W/mK

S =conduction shape factor

T =temperature, K

T_i =temperature of the inner surface, K

T_o =temperature of the outer surface, K

Y_k =unknown in the linear system

b_i =length scale used to divide any length to convert that length to dimensionless form

r =radial distance of any point from the origin of reference

Bi =Biot number

Greek symbols

Θ =dimensionless temperature

θ =angle

Subscripts

i =inner surface

o =outer surface

∞ =ambient

Contents

Supervisor’s Certificate	ii
Dedication	iii
Declaration of Originality	iv
Acknowledgment	v
Abstract	vi
Nomenclature	vii
List of Figures	ix
1 Introduction	2
1.1 Mathematical formulation	4
2 Results and Discussion	9
2.1 (Case-1):Heat exchanger tubes bounded by isothermal inner and isothermal outer noncircular cross-section	9
2.2 (Case-2):Heat exchanger tubes bounded by isothermal inner and convective outer noncircular cross-section	13
2.3 Validation	13
2.4 Error analysis	17
3 Conclusion and Scope for further work	20
References	22

List of Figures

1.1	cross-section of a heat exchannger tube	4
2.1	Temperature distribution in an exchanger tube of (a) both isothermal inner and outer circular cross-section (b) eccentric annuli of both isothermal inner and outer cross-section	10
2.2	(a) Temperature distribution and (b) schematics of a heat exchanger tube with outer rounded square cross-section and inner square cross-section . . .	11
2.3	(a) Temperature distribution and (b) schematics of a heat exchanger tube with flower like outer cross-section and inner square cross-section	11
2.4	(a) Temperature distribution and (b) schematics of a heat exchanger tube with outer elliptic cross-section and inner 8 sided polygonal cross-section .	11
2.5	(a) Temperature distribution and (b) schematics of a heat exchanger tube with outer elliptic cross-section and inner rounded square cross-section . . .	12
2.6	(a) Temperature distribution and (b) schematics of a heat exchanger tube with both inner and outer isothermal flower like cross-section	12
2.7	Temperature distribution in an exchanger tube of isothermal inner and convective outer (a) circular cross-sections (b) elliptic cross-sections	13
2.8	Temperature distribution in an exchanger tube with (a) outer convective rounded square cross-section and inner isothermal square cross-section (b) convective flower like outer cross-section and isothermal inner square cross-section	14
2.9	Temperature distribution in an exchanger tube with (a) convective outer elliptic cross-section and isothermal inner 8 sided polygonal cross-section (b) convective outer elliptic cross-section and isothermal inner rounded square cross-section	14
2.10	Temperature distribution in an exchanger tube with (a) inner isothermal and outer convective flower like cross-section (b) inner isothermal and outer convective eccentric annuli	14

2.11	Angular variation of temperature as a function of the radial distance for an exchanger tube of (a) outer rounded square cross-section and inner square cross-section (b) outer elliptic cross-section and inner octagonal cross-section	15
2.12	Comparison of analytical and numerical values of CSF for a heat exchanger with (a) outer square cross-section and inner circular cross-section (b) outer rectangular cross-section and inner circular cross-section	15
2.13	(a) Comparison of analytical and numerical values of CSF for an elliptic heat exchanger (b) Variation of percentage error in CSF calculation with the total number of collocation points	15
2.14	(a) Variation of percentage error in CSF calculation with the number of unknowns in equation (1.11) (b) Variation of global error with the number of unknowns in equation (1.11)	16
2.15	(a) Temperature determination along a line which is not a radius for a circular exchanger tube (b) Variation of percentage error in CSF calculation with eccentricity	16

List of Tables

2.1	Comparison of CSF value by BCM with the analytic CSF value	10
2.2	CSF valuefor different shapes considered from figure 2.2 to figure 2.6 . . .	13
2.3	CSF value of a circular heat exchanger for different eccentricity	19

Chapter 1

Introduction

Heat exchange tubes have many applications in diverse range of fields which include refrigeration and air conditioning, automotive, aerospace, cooling of gas turbine blades, power and process engineering and many more. Using exchanger tubes is one of the most effective ways of cooling microelectronics. Traditionally used exchanger tubes have circular cross-section because it is easily available and for a fixed perimeter, circular shape has the minimum area which in turn minimizes the material cost. But with the development of polymeric material and nanotechnology, we are able to manufacture exchanger tubes of different aerodynamic shapes.

In 1913, Langmuir et, al. [?] introduced the concept of Conduction Shape Factor (CSF). If the steady state temperatures at the two boundaries and the corresponding CSF for an exchanger tubes and are known, then the total heat flow can easily be calculated by $Q = K_t S (T_i - T_o)$ where S is the CSF defined as $S = \int_{\Gamma} \frac{\partial \Theta}{\partial n} d\Gamma$. Here Θ is the dimensionless temperature. Several researchers further extended Langmuir's idea of finding CSF [?], [?], [?], [?]. Determining CSF is one best way to investigate the heat conduction in two-dimensional domain. Some researchers have proposed different techniques for solving heat conduction problems for oval and elliptic shaped exchanger tubes [?], [?], [?]. Merker et, al. [?] investigated heat conduction in oval-shaped tubes experimentally and found out that oval-shaped tubes have smaller front areas on the shell-side as compared to those with the circular tubes. This helped to recover the waste heat from the exhaust of gas turbines. Kolodziej et, al. [?] suggested a semi-analytic technique to find the CSF of circular and polygonal cross-sections. Many literatures [?], [?], [?], [?], [?] have been reported which proved the advantage of using non-circular exchanger tubes over the traditional circular exchanger tubes. Bouris et, al. [?] showed that the elliptic exchanger tubes have lower rate of fouling and pressure drop but higher heat transfer rate as compared to circular exchanger tubes. Moharana et, al. [?] used the sector method and the boundary collocation method to improve the analysis done by Li et, al. [?]. They found that the boundary collocation method gives a more reliable and accurate solution as compared to the [?] fin analysis method. Moharana et, al. [?] also used boundary collocation method, sector method and the perturbation technique to study the

heat conduction in eccentric annuli and proposed its advantage in insulation. Many articles have been published on heat conduction through exchanger tubes of circular cross-section and exchanger tubes of outer circular cross-section and inner noncircular cross-section and exchanger tubes of inner circular cross-section and outer noncircular cross-section. Till date, no literature is available for heat conduction through exchanger tubes of both inner and outer noncircular cross-section. This dissertation presents an improved analysis of heat conduction in exchanger tubes of both inner and outer noncircular cross-section.

Figure 1.1 depicts a heat exchanger tubes of both inner and outer noncircular cross-section whose inner and outer surfaces are kept at constant but different temperatures. The problem considered here is a two-dimensional boundary value problem governed by the two-dimensional Laplace equation. We can solve this problem using finite difference method, finite element method and boundary element method. These methods are comparatively complex and the time required to generate the mesh using any of these methods is much higher as compared to boundary collocation method making these methods unreasonable to use. But using the boundary collocation method to solve this type of problem is an efficient way which reduces computational complexity as well as saves the important time. Due to these advantages, the boundary collocation method finds extensive application in continuous mechanics [?]. The brief overview of the paper is as follows:

- temperature profile for heat exchanger tubes bounded by isothermal inner and outer noncircular cross-section is found out
- temperature profile for heat exchanger tubes bounded by isothermal inner and convective outer noncircular cross-section is calculated
- CSF obtained by numerical methods is compared with the exact CSF to convey the reliability of the method.

1.1 Mathematical formulation

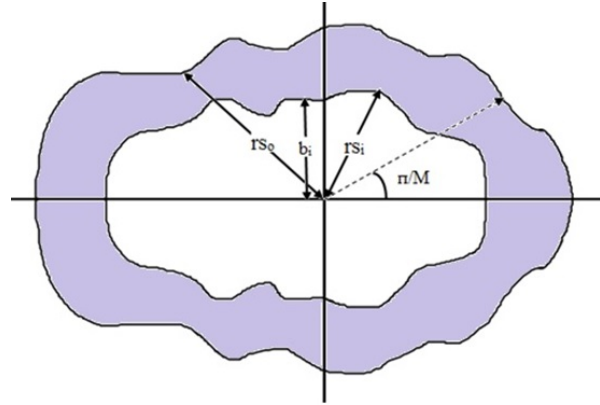


Figure 1.1: cross-section of a heat exchanger tube

The dimensionless parameters

$$\Theta = \frac{T - T_o}{T_i - T_o} \quad R = \frac{r}{b_i} \quad R_1 = \frac{r_{Si}}{b_i} \quad R_2 = \frac{r_{So}}{b_i}$$

where Θ , R , r_{Si} , r_{So} , r , b_i , T_i and T_o are the same as defined in the Nomenclature section.

i. Case-1: Heat exchanger tubes bounded by isothermal inner and outer noncircular cross-section

In Figure 1.1 the inner and outer boundaries are maintained at uniform temperatures T_i and T_o respectively. The domain is symmetric with respect to the angles $\theta = 0$ and $\theta = \frac{\pi}{M}$ where M is the number of symmetry of the cross-section about π . In this work, we solve the Laplace equation in polar form because using it gives us an advantage for computational purpose.

The two dimensional Laplace equation in dimensionless parameters is

$$\frac{\partial^2 \Theta}{\partial R^2} + \frac{1}{R} \frac{\partial \Theta}{\partial R} + \frac{1}{R^2} \frac{\partial \Theta}{\partial \theta} = 0. \quad (1.1)$$

The general solution of equation (1.1) is

$$\begin{aligned}
\Theta(R, \theta) = & A + B \ln R + C\theta + D\theta \ln R \\
& + \sum_{k=1}^{\infty} (A_k R^{\lambda_k} + B_k R^{-\lambda_k}) \cos(\lambda_k \theta) \\
& + \sum_{k=1}^{\infty} (C_k R^{\lambda_k} + D_k R^{-\lambda_k}) \sin(\lambda_k \theta).
\end{aligned} \tag{1.2}$$

Where A, B, C, D, C_k and D_k are constants to be determined.

The boundary conditions are

$$\frac{\partial \Theta}{\partial \theta} = 0 \quad \text{for } \theta = 0. \tag{1.3}$$

$$\frac{\partial \Theta}{\partial \theta} = 0 \quad \text{for } \theta = \frac{\pi}{M}. \tag{1.4}$$

where M is the number of symmetry about π .

$$\Theta = 1 \quad \text{for } R = R_1. \tag{1.5}$$

$$\Theta = 0 \quad \text{for } R = R_2. \tag{1.6}$$

Differentiating equation (1.2) with respect to θ and then applying equation (1.3) yields

$$C = D = C_k = D_k = 0. \tag{1.7}$$

Again differentiating equation (1.2) with respect to θ and then applying equation (1.4) we get

$$\lambda_k = kM. \tag{1.8}$$

Substituting (1.7) and (1.8) in (1.2) results in

$$\Theta(R, \theta) = A + B \ln R + \sum_{k=1}^{\infty} (A_k R^{Mk} + B_k R^{-Mk}) \cos(Mk\theta). \tag{1.9}$$

Reducing the number of modes to $p - 1$ equation (1.9) can be rewritten as

$$\Theta(R, \theta) = A + B \ln R + \sum_{k=1}^{p-1} (A_k R^{Mk} + B_k R^{-Mk}) \cos(Mk\theta). \tag{1.10}$$

Introducing new variables

$$Y_1 = A, Y_2 = A_2, Y_3 = A_2, \dots, Y_p = A_{p-1},$$

$$Y_{p+1} = B, Y_{p+2} = B_1, Y_{p+3} = B_2, \dots, Y_{2p} = B_{p-1}$$

So (1.10) can be written as

$$\Theta(R, \theta) = \sum_{k=1}^{2p} Y_k \Psi_k(R, k, \theta). \quad (1.11)$$

where

$$\Psi_1 = 1 \text{ and } \Psi_k = R^{M(k-1)} \cos(M(k-1)\theta) \text{ for } k = 2, 3, \dots, p$$

$$\Psi_{p+1} = \ln R \text{ and } \Psi_k = R^{-M(k-p-1)} \cos(M(k-p-1)\theta) \text{ for } k = p+2, p+3, \dots, 2p.$$

Now boundary collocation method will be used to solve this problem.

ii. Boundary Collocation Method(BCM)

The boundary collocation method is a method that satisfies the general solution of the governing differential equation of the problem at a finite number of points along the boundary rather than using the general solution of the governing differential equation along the whole boundary. The details of this method can be found in the book Kolodziej et, al[17]. There is no heat conduction in the axial direction and the problem is investigated when the domain is at steady state. Temperature is different but uniform and constant at both the inner and outer surfaces. There is no internal heat generation in the material of the exchanger tube. The thermal conductivity of the material of the tube is constant throughout the domain. These are the assumptions made by the authors before applying the boundary collocation method. Now we apply BCM for $2N$ points i.e. N points on the inner boundary and N points on the outer boundary. Hence we have $2p$ unknowns and $2N$ number of equations. So (1.11) forms a system of equations $ZY = b$ where Z is the coefficient matrix of order $2N \times 2p$, Y is the vector of order $2p \times 1$ and contains the unknowns Y_k s and finally b is a column vector of order $2N \times 1$. Now using equation (1.5) we can write equation (1.11) as

$$\sum_{k=1}^{2p} Y_k \Psi_k(R_1, k, \theta) = 1. \quad (1.12)$$

Using equation (1.6) and equation (1.11) we can obtain

$$\sum_{k=1}^{2p} Y_k \Psi_k(R_1, k, \theta) = 0. \quad (1.13)$$

Solving equation (1.12) and equation (1.13) we can determine the values of all the

unknown Y_k s.

iii. **Case-2: Heat exchanger tubes bounded by isothermal inner and convective outer noncircular cross-section**

The boundary conditions are

$$\frac{\partial \Theta}{\partial \theta} = 0 \quad \text{for } \theta = 0. \quad (1.14)$$

$$\frac{\partial \Theta}{\partial \theta} = 0 \quad \text{for } \theta = \frac{\pi}{M}. \quad (1.15)$$

$$\Theta = 1 \quad \text{for } R = R_1. \quad (1.16)$$

$$\frac{\partial \Theta}{\partial R} + Bi^* \Theta = 0 \quad \text{for } R = R_2. \quad (1.17)$$

Where $Bi^* = \frac{Bi * b_i}{r}$

Using equations (1.2), (1.14) and (1.15) we obtain $C = D = C_k = D_k = 0$ and $\lambda_k = kM$. Hence, equation (1.2) can be written as

$$\Theta = A + B \ln R + \sum_{k=1}^{\infty} (A_k R^{Mk} + B_k R^{-Mk}) \cos(Mk\theta). \quad (1.18)$$

Reducing the number of modes to $p - 1$ equation (1.18) can be rewritten as

$$\Theta = A + B \ln R + \sum_{k=1}^{p-1} (A_k R^{Mk} + B_k R^{-Mk}) \cos(Mk\theta). \quad (1.19)$$

From equation (1.16) and equation (1.19)

$$A + B \ln R + \sum_{k=1}^{p-1} (A_k R_1^{Mk} + B_k R_1^{-Mk}) \cos(Mk\theta) = 1. \quad (1.20)$$

Introducing new variables as in the previous case, we get

$$\sum_{k=1}^{2p} Y_k \Psi_k(R_1, k, \theta) = 1. \quad (1.21)$$

Where

$\Psi_1 = 1$ and $\Psi_k = R_1^{M(k-1)} \cos(M(k-1)\theta)$ for $k = 2, 3, \dots, p$

$\Psi_{p+1} = \ln R$ and $\Psi_k = R_1^{-M(k-p-1)} \cos(M(k-p-1)\theta)$ for $k = p+2, p+3, \dots, 2p$

Equation (1.16) is satisfied when

$$\sum_{k=1}^{p-1} Y_k \Psi_k(R_1, k, \theta) = 1. \quad (1.22)$$

Considering only $p - 1$ number of modes, equation (1.17) is satisfied when

$$\begin{aligned} \frac{B}{R_2} + \sum_{k=1}^{p-1} Mk [A_k R_2^{Mk-1} - B_k R_2^{-Mk-1}] \cos(Mk\theta) \\ + Bi^* [A + B \ln R_2 \sum_{k=1}^{p-1} (A_k R_2^{Mk} - B_k R_2^{-Mk}) \cos(Mk\theta)] = 0. \end{aligned} \quad (1.23)$$

Equivalently we can write equation (1.24) as follows

$$\sum_{k=1}^{2p} Y_k \Psi_k(R_1, k, \theta) = 0. \quad (1.24)$$

Here

$$\Psi_1 = Bi^*$$

$$\Psi_k = [M(k-1)R_2^{M(k-1)-1} + Bi^* R_2^{M(k-1)-1}] \cos(M(k-1)\theta) \text{ for } k = 2, 3, \dots, p$$

$$\Psi_{p+1} = Bi^* \ln R_2 + \frac{1}{R_2}$$

$$\Psi_k = [-M(k-p-1)R_2^{-M(k-p-1)-1} + Bi^* R_2^{-M(k-p-1)}] \cos(M(k-p-1)\theta) \text{ for } k = p+2, p+3, \dots, 2p$$

Writing equation (1.22) at N points on the inner boundary and writing equation (1.24) at N points on the outer boundary, we can form a simultaneous system of equations as in the previous case. By solving this system of equations, we can obtain all the unknowns. Once we obtain the value of the unknowns, we can determine the dimensionless temperature at any point inside the domain.

Chapter 2

Results and Discussion

In this chapter, heat conduction for various geometrical shapes as well as for some standard geometrical shapes has been solved. The standard geometrical shapes for which analytical solutions are available is used to validate the results of boundary collocation method. For all the geometrical shapes considered in this paper the CSF can be calculated by

$$\begin{aligned} S &= \int_{\Gamma} \frac{\partial \Theta}{\partial \eta} d\Gamma \\ &= - \int_0^{2\pi} \frac{\partial \Theta}{\partial R} R d\Theta \\ &= - \int_0^{2\pi} B d\Theta - \int_0^{2\pi} \sum_{k=1}^{p-1} M k (A_k R^{Mk} - B_k R^{-Mk}) \cos(Mk\theta) d\Theta \\ &= -2\pi B \\ &= -2\pi Y_{p+1} \end{aligned}$$

2.1 (Case-1): Heat exchanger tubes bounded by isothermal inner and isothermal outer noncircular cross-section

Figure 2.1(a) shows the heat conduction for a heat exchanger tube of both inner and outer circular cross-section. The problem has been solved for the steady state considering constant inner temperature T_i and constant outer temperature T_o . These values of T_i and T_o are considered for all other geometrical shapes solved in this literature. In [18], the analytical expression for heat exchanger tube of both inner and outer cross-section is given [?] by

$$S = \frac{2\pi L}{\ln(r_o/r_i)}. \quad (2.1)$$

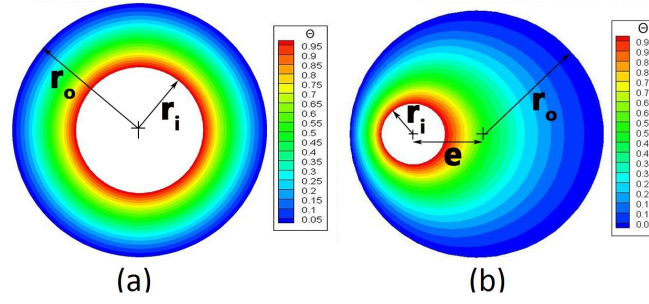


Figure 2.1: Temperature distribution in an exchanger tube of (a) both isothermal inner and outer circular cross-section (b) eccentric annuli of both isothermal inner and outer cross-section

where L is the length in the axial direction. Figure 2.1(b) shows the temperature profile for an eccentric annuli with eccentricity 2 and $r_o/r_i = 4$. While solving this problem, the origin of the frame of reference is chosen at a distance of from the centre of the inner circular surface towards the centre of the outer circular surface. Hence with respect to the author's choice of frame of reference both the surfaces of the annuli are noncircular. In [?] the shape factor for this type of eccentric annuli is given by

$$S = \frac{2\pi L}{\cosh^{-1}[(r_o^2 + r_i^2)/2r_o r_i]}. \quad (2.2)$$

Equation (2.1) and (2.2) can be used to find out the numerical values of CSF for both the circular shape and eccentric annuli presented in the Figure 2.1(a) and Figure 2.1(b). The problem for both the shapes in Figure 2.1 and Figure 2.2 have been solved for the purpose of validation of the boundary collocation method. From Table 2.1, it is clear that the boundary collocation method gives pretty good approximate solution and hence, we can rely on this method.

Table 2.1: Comparison of CSF value by BCM with the analytic CSF value

Geometrical shape	r_o/r_i	CSF- Analytical	CSF-BCM
Circular	2	9.064720284	9.064751443
Eccentric annuli	4	5.890123070	5.888601269

Figure 2.2 shows the teperature distribution in a heat exchanger tube with outer rounded square cross-section and inner square cross-section. This shape is one of the most commonly used shape for exchanger tubes. For this figure, the ratio of $a_o/a_i = 2$ was considered. Although the inner surface has corners with angle 90^0 , the method was able to give good results. The CSF for this shape was found to be 4.785902248. In Figure 2.3, a_o and a_i are taken as 3 and 2 respectively. Figure 2.2(a), Figure 2.3(a) and Figure 2.4(a) show the ability of the method to handle boundaries with sharp corners

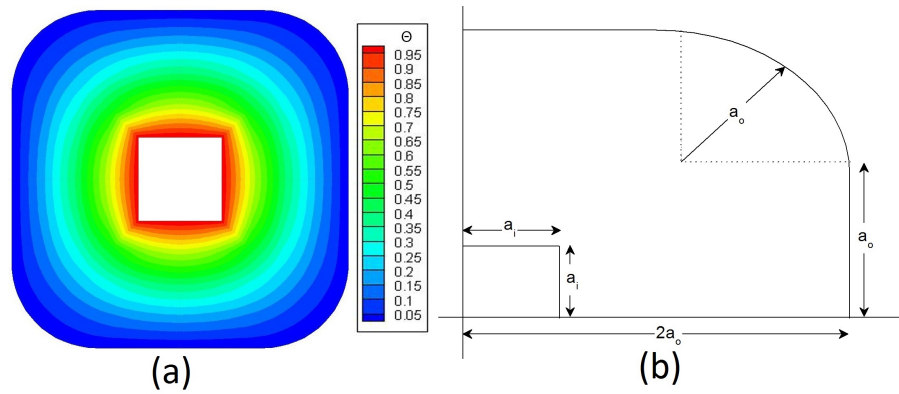


Figure 2.2: (a) Temperature distribution and (b) schematics of a heat exchanger tube with outer rounded square cross-section and inner square cross-section

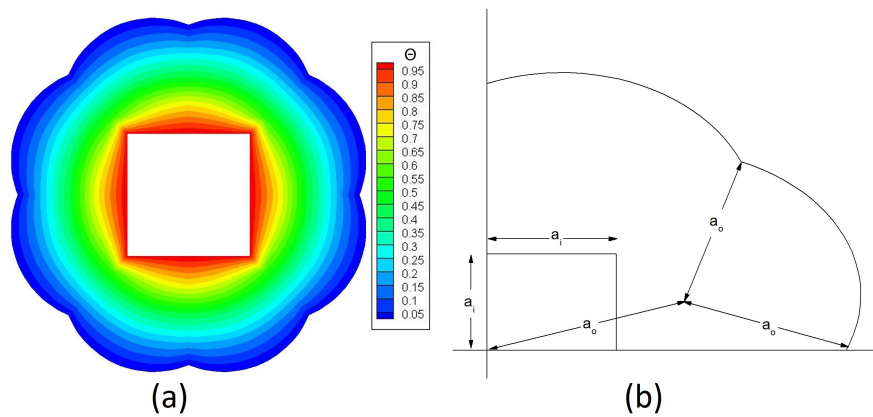


Figure 2.3: (a) Temperature distribution and (b) schematics of a heat exchanger tube with flower like outer cross-section and inner square cross-section

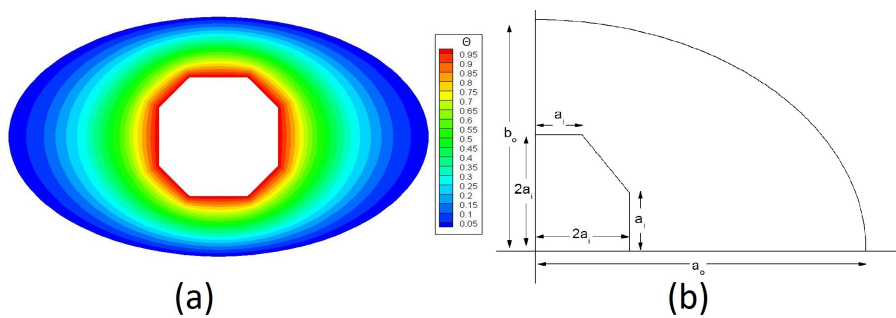


Figure 2.4: (a) Temperature distribution and (b) schematics of a heat exchanger tube with outer elliptic cross-section and inner 8 sided polygonal cross-section

with angles 90° or more than 90° . But, if both the two boundaries have boundaries with sharp corners of angle 90° or less than 90° the method may fail to give correct results.

Several investigations have established the potential of using elliptic shapes in the design of various heat exchanger tubes. Many authors have also shown the superiority

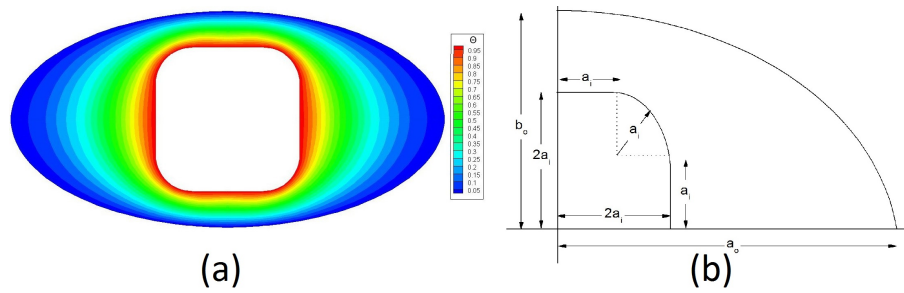


Figure 2.5: (a) Temperature distribution and (b) schematics of a heat exchanger tube with outer elliptic cross-section and inner rounded square cross-section

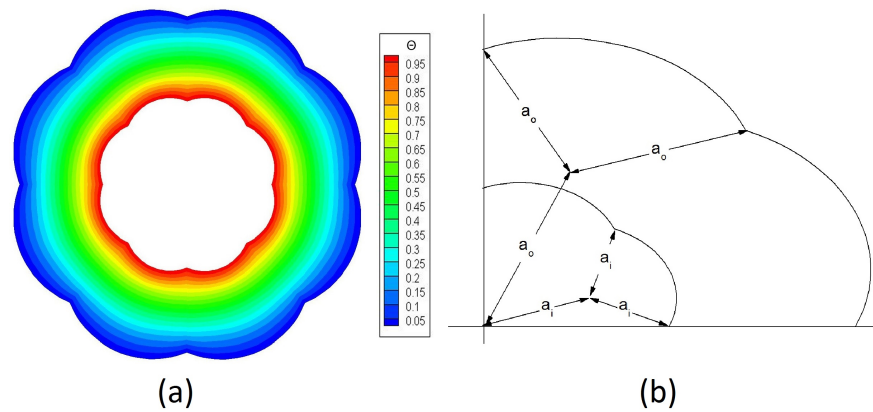


Figure 2.6: (a) Temperature distribution and (b) schematics of a heat exchanger tube with both inner and outer isothermal flower like cross-section

of elliptic tubes in drag reduction and its advantage in cross-flow. Hence, we felt the necessity of investigating the combination of elliptic shape with other shapes. Figure 2.4 presents the heat conduction analysis of an exchanger tube with outer elliptic cross-section and inner 8 sided polygonal cross-section. The heat conduction problem has been solved considering $a_i = 1$ and $a_o = 7$ and $b_o = 4$. Figure 2.5 displays the heat conduction of an exchanger tube with outer elliptic cross-section and inner rounded square cross-section. For the problem in Figure 2.5, the values of a_i , a_o , b_o are chosen as 1, 6 and 3 respectively. In Figure 2.6, a flower like shape having 8 number of symmetry is considered. The heat conduction problem for this shape is solved by taking $a_i = 1$ and $a_o = 2$ and then using boundary collocation method. The results obtained from this analysis are satisfactory.

Table 2.2: CSF value for different shapes considered from figure 2.2 to figure 2.6

Geometrical shape in	Numerical value of CSF
Figure 2.2	4.785902248
Figure 2.3	6.839875525
Figure 2.4	7.788335961
Figure 2.5	7.788335961
Figure 2.6	9.171086768

2.2 (Case-2): Heat exchanger tubes bounded by isothermal inner and convective outer noncircular cross-section

Some geometrical shapes have been considered where the problem has been solved for conjugate heat transfer i.e. conduction with convection and are presented in figure 2.7 to Figure 2.10. From the present analysis, it is quite convincing that heat conduction problems for complicated geometries can be easily handled by boundary collocation method.

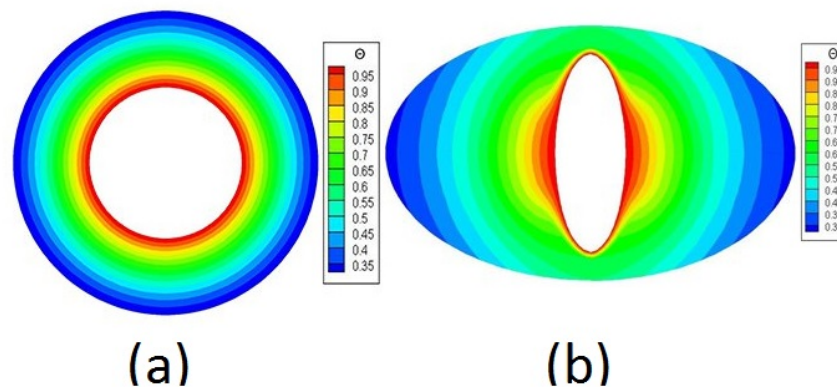


Figure 2.7: Temperature distribution in an exchanger tube of isothermal inner and convective outer (a) circular cross-sections (b) elliptic cross-sections

2.3 Validation

We represent the obtained results in Figure 2.11 for the purpose of analysis. Figure 2.11(a) shows the angular variation of temperature as a function of the radial distance for an exchanger tube of outer rounded square cross-section and inner square cross-section. Here T_i and T_o are considered to be 80° and 20° respectively. With the increasing radial distance, the angular variation gradually deviates from the uniform

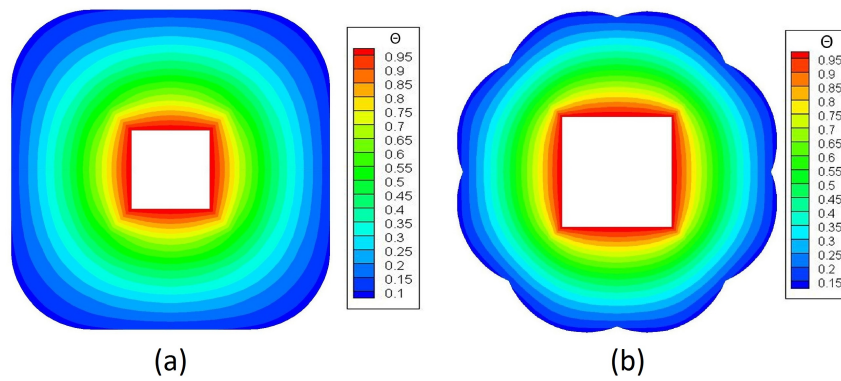


Figure 2.8: Temperature distribution in an exchanger tube with (a) outer convective rounded square cross-section and inner isothermal square cross-section (b) convective flower like outer cross-section and isothermal inner square cross-section

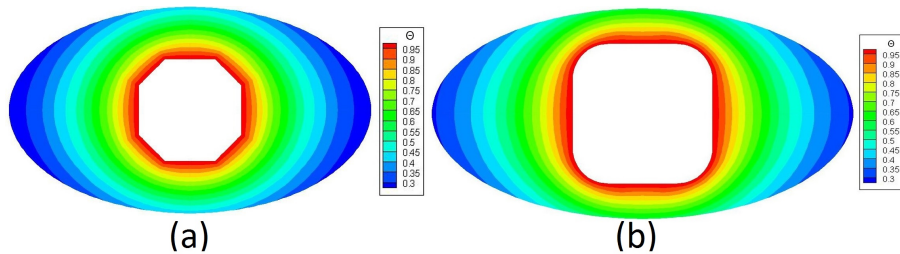


Figure 2.9: Temperature distribution in an exchanger tube with (a) convective outer elliptic cross-section and isothermal inner 8 sided polygonal cross-section (b) convective outer elliptic cross-section and isothermal inner rounded square cross-section

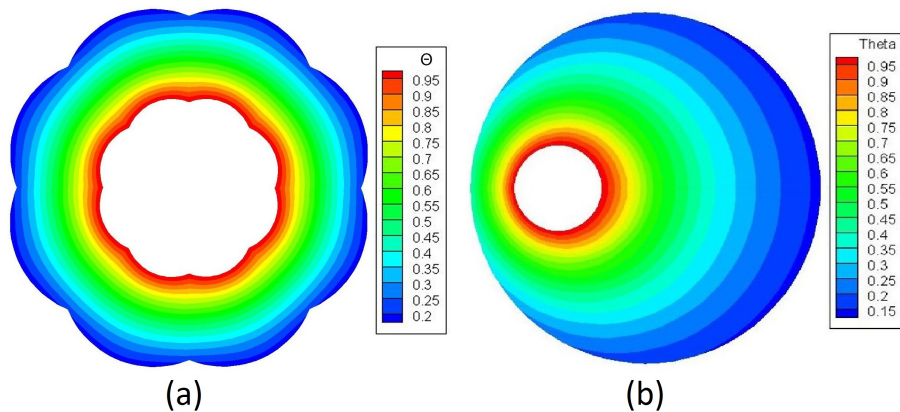


Figure 2.10: Temperature distribution in an exchanger tube with (a) inner isothermal and outer convective flower like cross-section (b) inner isothermal and outer convective eccentric annuli

distribution. As we go from angle 0^0 to angle 45^0 , the thickness in the radial direction increases which makes the curve the steepest at angle 0^0 . Since we have considered a combination of outer rounded square cross-section and inner square cross-section, the thickness in the radial direction does not change much with variation of the angle and

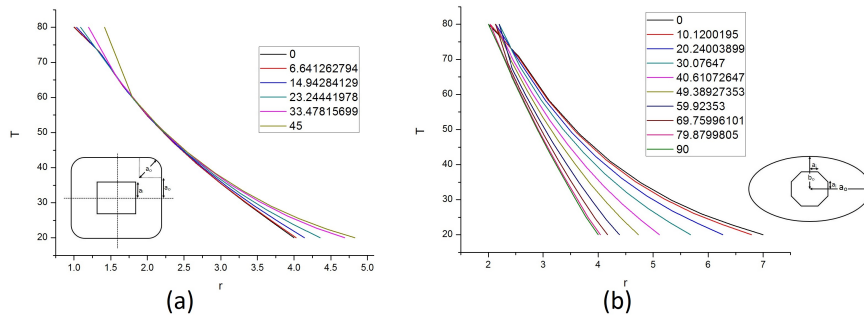


Figure 2.11: Angular variation of temperature as a function of the radial distance for an exchanger tube of (a) outer rounded square cross-section and inner square cross-section (b) outer elliptic cross-section and inner octagonal cross-section

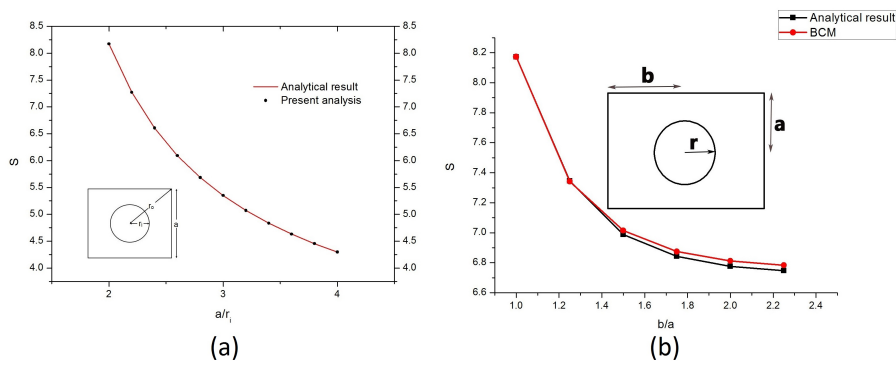


Figure 2.12: Comparison of analytical and numerical values of CSF for a heat exchanger with (a) outer square cross-section and inner circular cross-section (b) outer rectangular cross-section and inner circular cross-section

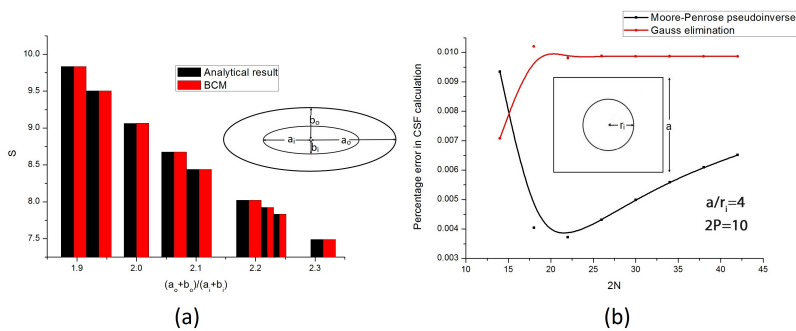


Figure 2.13: (a) Comparison of analytical and numerical values of CSF for an elliptic heat exchanger (b) Variation of percentage error in CSF calculation with the total number of collocation points

that's why we got a region in the middle portion where the temperature distribution is uniform for every angle. In Figure 2.11(b), the temperature versus the radial distance from the origin of reference is plotted for different angles. One can observe that the temperature distribution is dependent on the thickness of the exchanger tube. The

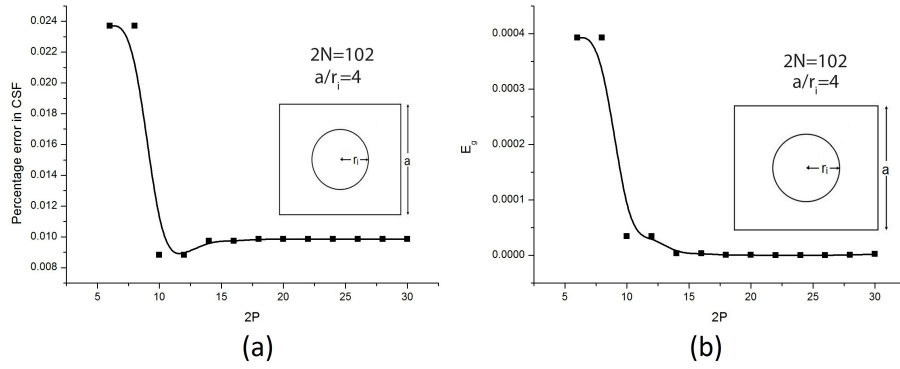


Figure 2.14: (a) Variation of percentage error in CSF calculation with the number of unknowns in equation (1.11) (b) Variation of global error with the number of unknowns in equation (1.11)

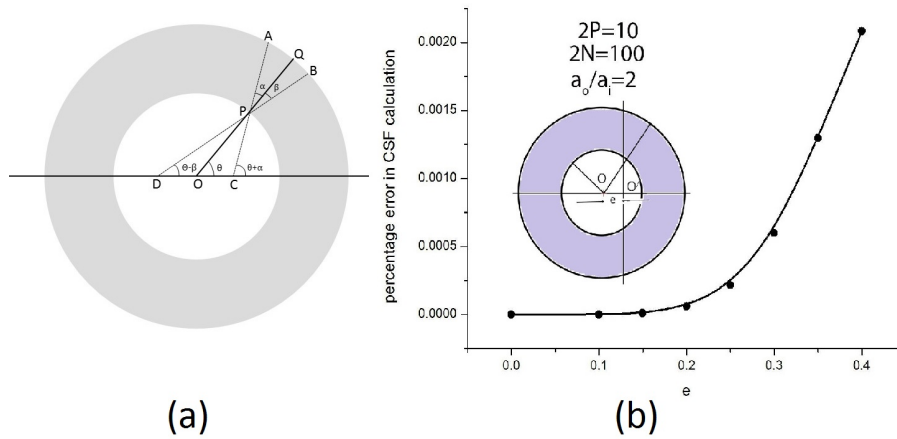


Figure 2.15: (a) Temperature determination along a line which is not a radius for a circular exchanger tube (b) Variation of percentage error in CSF calculation with eccentricity

figure is drawn considering $a_i = 1, a_o = 7, b_o = 4$. Here, the thickness decreases as the value of the angle increases. So the temperature at a higher angle is higher for the same radial distance making the curve steeper at a higher angle. Thus, we get the maximum steepness at the angle 90° and minimum steepness at the angle 0° .

A comparison between the analytical value of CSF and the value of CSF obtained by BCM is presented for a domain with outer square cross-section and inner circular cross-section in figure 2.12(a). The length of the side of the square is increased keeping the radius of the inner circle fixed. For such cases, the value of CSF is plotted against a/r where a is length of the side of the outer square cross-section and r is radius of the inner circular cross-section. The CSF value can be determined analytically [?] by

$$S = \frac{2\pi L}{\ln(r_o/r_i) - 0.27079} \tag{2.3}$$

A comparison between the analytical value of CSF and the value of CSF obtained by

BCM is presented for a domain with outer rectangular cross-section and inner circular cross-section in Figure 2.12(b). The length of the rectangle is increased keeping the breadth of the rectangle and the radius of the inner circle fixed. For such cases, the value of CSF is plotted against b/a where a is the breadth of the outer rectangular cross-section and b is the length of the outer rectangular cross-section. The analytical CSF value for such a geometry can be obtained [?] by

$$S = \frac{2\pi L}{\ln(4a/\pi r) - 2l}. \quad (2.4)$$

Here l is the correction term as defined by Balcerzak and Raynor [?]. In Figure 2.13(a), an exchanger tube of both inner and outer elliptic cross-sections is considered and the values of CSF is plotted against $(a_o + b_o)/(a_i + b_i)$. The values of a_i and a_o are the major axes of the inner and outer ellipses respectively. b_i and b_o are the minor axes of the inner and outer ellipses respectively. The analytical expression CSF for such an exchanger tube is given [?] by

$$S = \frac{2\pi L}{\ln((a_o + b_o)/(a_i + b_i))}. \quad (2.5)$$

The value of a_i and b_i are kept constant. Then a_o and b_o are chosen so that both the inner and outer ellipses will be confocal. For such a case, when the shape of the ellipses becomes more and more circular means the distance between the two foci tends to zero, the CSF obtained by the present analysis tend to match more accurately with the analytical result *i.e.* the difference between the analytical and numerical value of CSF tends to zero. The excellent agreement of the solution obtained by the proposed method with the analytical solution shows that we can certainly rely on the BCM.

2.4 Error analysis

The global error can be calculated as follows.

$$E_g = \frac{1}{2N} \sum_{i=1}^{2N} [\Theta_e(R_i, \theta_i) - \Theta_a(R_i, \theta_i)]^2. \quad (2.6)$$

where E_g represents the global error. $\Theta_e(R_i, \theta_i)$ and $\Theta_a(R_i, \theta_i)$ are the exact value of dimensionless temperature given by the boundary condition and numerical value of dimensionless temperature arising from BCM respectively. R_i and θ_i are the dimensionless radius and angle of the i -th collocation point where the boundary condition is fulfilled approximately. $2N$ is the total number of collocation points considered in the inner and outer boundaries of the domain. The local error can be

found as

$$(E_l)_i = |\Theta_e(R_i, \theta_i) - \Theta_a(R_i, \theta_i)|. \quad (2.7)$$

where $(E_l)_i$ is the local error at the i -th collocation point. The local error is bounded by E which means that $(E_l)_i \leq E$ for $i = 1, 2, \dots, 2N$.

where $E = \max_{i=1}^{2N} |\Theta_e(R_i, \theta_i) - \Theta_a(R_i, \theta_i)|$

Hence, the value of $\Theta_a(R_i, \theta_i)$ lies in the interval $[\Theta_e(R_i, \theta_i) - E, \Theta_e(R_i, \theta_i) + E]$.

The system of equations obtained from BCM is solved using Gauss elimination and Moore-Penrose pseudoinverse. When $2N = 2p$, we solve the system using Gauss elimination method. But, when $2N > 2p$, we solve the system using pseudoinverse method. The percentage error for CSF calculation is obtained for both Gauss elimination and pseudoinverse method and is presented in Figure 2.13(a). It is clear from the figure that the pseudoinverse method gives less error as compared to the Gauss elimination method for the same number of collocation points. Moreover, when the number of collocation points is high, the matrix obtained from the system of equations becomes ill-conditioned. Hence, solving such a system using Gauss elimination may produce biased results. This problem can be avoided by using the pseudoinverse method. Hence, the authors felt the necessity of using the pseudoinverse method.

Since, we are solving a second order Laplace equation, we need two boundary conditions to obtain the solution. But due to the presence of a complicated geometry, we are not able to obtain the solution analytically and hence, adopting numerical methods to obtain the complete solution. From the numerical solution, it can be verified that the unknown constants in the summation term has much less contribution towards the solution as compared to the unknown constants outside the summation term in equation (1.10) and equation (1.20). Hence, considering a large number of terms in the summation series does not affect the solution much. So the authors preferred the pseudoinverse method to the Gauss elimination method. A comparative study of how the CSF value is affected by varying the number of terms in the summation in equation (1.11) is presented in Figure 2.14(a). It is observed that 10 number of unknown constants in equation (1.11) gives the minimum percentage error in CSF calculation and the error almost remains constants for higher number of unknown constants. Hence, 10 is the optimum number of unknown constants in equation (1.11) for CSF calculation for the considered geometry in the Figure 2.14(a). Figure 2.14(b) shows the change of the global error as defined earlier with respect to the change of the value of $2p$. The global error decreases for low values of $2p$ but it is almost equal to zero for higher values of $2p$. We can say that for higher values of $2p$ the method is stabilised. So it is clear from Figure 2.13(a), 2.13(b) and 2.14(a) that the domain of any smooth geometry can be easily handled with

BCM and pseudoinverse method. In Figure 2.15(a), O is the origin of the frame of reference. Several methods are available which can determine the temperature distribution along line PQ. But so far, no numerical method is designed to obtain the temperature distribution along the line PA or PB. But this can be done by BCM. If we shift the origin of the frame of reference from O to C , the line AB falls in the radial direction of the newly considered origin. Hence, $OC = a_i \sin(\theta) / \tan(\theta + \alpha)$ and $e = a_i \cos(\theta) - a_i \sin(\theta) / \tan(\theta + \alpha)$. Considering this eccentricity, the problem can be solved to get the temperature distribution along the line PA at an angle of $\theta + \alpha$. Similarly the temperature distribution along line PB can be calculated considering $e = a_i \sin(\theta) / \tan(\theta - \beta) - a_i \cos(\theta)$ in the negative x-axis and at an angle of $\theta - \beta$.

Table 2.3: CSF value of a circular heat exchanger for different eccentricity

e	CSF-BCM	CSF- Analytical	Percentage error
0	9.064720284	9.064720284	0
0.1	9.064720368	9.064720284	9.27E-07
0.15	9.064721246	9.064720284	1.06E-05
0.2	9.064725614	9.064720284	5.88E-05
0.25	9.064739904	9.064720284	0.000216
0.3	9.064774581	9.064720284	0.000599
0.35	9.064837709	9.064720284	0.001295
0.4	9.064909097	9.064720284	0.002083

Table 2.3 represents the variation of CSF with eccentricity . As we increase the value of e , the percentage error in the calculation of CSF increases. But the error is very small. Hence, we can obtain the value of CSF with high accuracy. From Table 2.3 and figure 2.15(b), we conclude that the BCM method can correctly predict the CSF value even if we shift the origin of the frame of reference from O to O' .

Chapter 3

Conclusion and Scope for further work

The method is highly dependent on the shape of the cross-section of the exchanger tubes. This method can handle cross-sections with smooth boundaries but it may fail to handle cross-sections with sharp edges. If the angle of this sharp edge is less than or equal to 90^0 , the method may fail to handle such a boundary. Figure 2.2(a), 2.3(a) and 2.4(a) clearly shows that up to some extent, this method can handle sharp edges, but if we consider an exchanger tube of both inner and outer cross-section having edges with angle 90^0 or less than 90^0 e.g. exchanger tube of both inner and outer rectangular cross-sections, this method may not give us correct results. So far, the method have been able to handle geometrical shapes if sharp edges with angle 90^0 or greater than 90^0 are present on any one boundary.

For all the cases considered, the number of collocation points chosen are close to 100 or more than 100. If the number of collocation points is less, the solution may be unsatisfactory. Moreover, if the number of points is very large, it may lead to a highly ill-conditioned system. For a better overview of this problem, one may refer Moharana et al [20]. Hence 100 collocation points are chosen as benchmark which is sufficient to give very good results but not large enough to give biased results. In the method adopted by the author, equidistant points on the boundaries are not chosen, rather points on the boundaries are chosen on the basis of equal angular distance. If we consider equidistant points on the boundaries, the computational complexity and the time required to do that may ruin the sole purpose of this paper. The proposed method based on boundary collocation technique was developed in this paper to numerically solve the two dimensional Laplace equation which is the governing differential equation for heat conduction in two dimensional domain. By the proposed method, there is no need to do huge and time consuming computational work. The excellent agreement between the obtained result and the exact solution presented in table 1 approve that the method is reliable. All the computational work

and calculations are done using MATLAB. The figures are generated using Tecplot and OriginLab.

This work can be further extended to solve three dimensional steady heat conduction problems. In that case, the three dimensional Laplace equation is used as the governing differential equation. All the boundary conditions used for this work are valid for that case. Some new boundary conditions arise for that case. All the boundary conditions are used to get the complete solution of the problem.

References

- [1] I. Langmuir, "Convection and radiation of heat," *Transaction of American Electrochemical Society*, vol. 23, no. 2, pp. 91 – 110, August 1913.
- [2] J. E. Smith, J.C. and Lind and D. S. Lermond, "Shape factors for conductive heat flow," *AICHE Journal*, vol. 4, no. 3, pp. 330 – 331, September 1958.
- [3] P. Laura and E. A. Susemihl, "Determination of heat flow shape factors for hollow regular polygonal prisms," *Nuclear Engineering and Design*, vol. 25, no. 3, pp. 409 – 412, August 1973.
- [4] L. Simeza and M. M. Yovanovich, "Shape factors for hollow prismatic cylinders bounded by isothermal inner circles and outer regular polygons," *International Journal of Heat and Mass Transfer*, vol. 30, no. 4, pp. 812 – 816, April 1987.
- [5] A. Hassani and K. Hollands, "Conduction shape factors for region of uniform thickness surrounding a three-dimensional body of arbitrary shape," *Journal of Heat Transfer*, vol. 112, no. 2, pp. 492 – 495, May 1990.
- [6] M. El-Saden, "Heat conduction in an eccentrically hollow, infinitely long cylinder with internal heat generation," *ASME Journal of Heat Transfer*, vol. 83, no. 4, pp. 510 – 512, November 1961.
- [7] R. F. DiFelice and H. H. Bau, "Conductive heat transfer between eccentric cylinders with boundary conditions of the third kind," *ASME Journal of Heat Transfer*, vol. 105, no. 3, pp. 678 – 680, August 1983.
- [8] M. A. I. El-Shaarawi and E. Mokheimer, "Transient conduction in eccentrically hollow cylinders," *International Journal of Heat and Mass Transfer*, vol. 38, no. 11, pp. 2001 – 2010, July 1995.
- [9] M. G.P. and H. H., "Heat transfer and pressure drop on the shell-side of the tube-banks having oval shaped tubes," *International Journal of Heat and Mass Transfer*, vol. 29, no. 12, pp. 1903 – 1909, December 1986.
- [10] J. Kolodziei and S. T., "Analytical approximations of the shape factors for conductive heat flow in circular and regular polygonal cross-sections," *International Journal of Heat and Mass Transfer*, vol. 44, no. 1, pp. 999 – 1012, November 1999.
- [11] B. D., P. G., and B. G., "Numerical evaluation of alternate tube configurations for particle deposition rate reduction in heat exchanger tube bundles," *International Journal of Heat and Fluid Flow*, vol. 22, no. 5, pp. 525 – 536, October 2001.
- [12] M. S. Abou-Dina, "Implementation of trefftz method for the solution of some elliptic boundary value problems," *Applied Mathematics and Computation*, vol. 127, no. 1, pp. 125 – 147, March 2002.

- [13] L. Z., D. J.H., and M. S.C, “Heat transfer enhancement using shaped polymer tubes:fin analysis,” *Journal of Heat Transfer*, vol. 127, no. 2, pp. 211 – 218, April 2004.
- [14] M. M. K. and D. P.K, “Heat conduction through heat exchanger tubes of noncircular cross-section,” *ASME Journal of Heat Transfer*, vol. 130, no. 1, pp. 301 – 309, January 2008.
- [15] M. Maharana1 and D. P.K., “Heat conduction through eccentric annuli: An appraisal of analytical, semi-analytical, and approximate techniques,” *ASME Journal of Heat Transfer*, vol. 134, no. 9, pp. – , March 2012.
- [16] K. Kolodziej, “Review of application of boundary collocation methods in mechanics of continuous media,” *Solid Mechanics Archives*, vol. 12, no. 4, pp. – , January 1987.
- [17] H. D.W. and O. M.N., *Heat Conduction*, 2012.
- [18] F. P. Incropera and D. P. DeWitt, *Introduction to Heat Transfer*. Wiley, New York, 1996.
- [19] B. M.J. and R. S., “steady state temperature distribution and heat flow in prismatic bars with isothermal boundary conditions,” *International Journal of Heat and Mass Transfer*, vol. 3, no. 2, pp. 113 – 125, September 1961.